*35th EPS Conference on Plasma Phys. Hersonissos, 9 - 13 June 2008 ECA Vol.**32D**, P-4.043 (2008)*

Analysis of the plasma periphery fluctuation parameters measured by multipin Langmuir probes near LCFS on the FT-2 Tokamak

S.I. Lashkul, S.V. Shatalin*, P.V. Vazhnov*, E.O. Vekshina*, L.A. Esipov, M.Yu. Kantor, D.V. Kouprienko, A.Yu. Popov, J. Vicente**

A.F.Ioffe Physico-Technical Institute, Politekhnicheskaya 26, 194021, St. Petersburg, Russia, Serguey.Lashkul@mail.ioffe.ru

**St.Petersburg State Polytechnical University, St. Petersburg, Russia*

***Ghent University, Gent, Belgium*

The effect of L-H transition during Lower Hybrid Heating (LHH) experiments was observed on the FT-2 tokamak. Change of the transport process at the plasma periphery during additional LHH (when external transport barrier (ETB) following the internal transport barrier (ITB) formation) was studied early in detail at P_{LHH} ~ 100kW [1]. The main attention has been on the self-consistence interaction of the edge and hot plasma core during ITB and ETB formation. Analysis of the plasma periphery fluctuation parameters measured by multipin Langmuir probes near LCFS show that L-H transition results in significant changes on the statistical characteristics of the periphery fluctuations. The PDFs of the investigated values are peaked and become more symmetrical in the LCFS vicinity [2, 3].

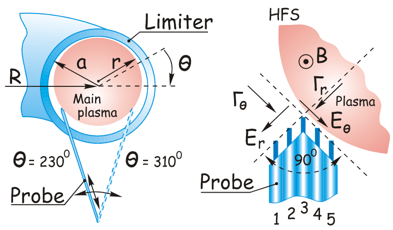

Fig. 1. *Multielectrode Langmuir probe arrangement for measurement at Low (LFS, $\theta = 310^0$) and High (HFS, $\theta = 230^0$) Field Sides of characteristic properties of periphery plasma parameters.*

This paper deals with new experiments with enhanced LHH power (P_{LHH} ~ 180kW) and new experimental techniques. The plasma periphery parameters are measured at two positions of the cross-section poloidal angle θ. The poloidal angle θ shows the probe position in respect to the equatorial outboard mid plane direction of the electron diamagnetic drift. The experimental scenario and multi pin Langmuir probe arrangement (shown in Fig. 1) for measurement of the periphery plasma parameters at Low (LFS, $\theta = 310^0$) and High (HFS, $\theta = 230^0$) Field Sides are described in detail in [1, 2]. Spatial and temporal characteristics of the peripheral plasma fluctuations were investigated by probe measurements in a vicinity of the LCFS. The probes can be moved shot by shot from limiter shadow and SOL (r ~ 80 – 76mm) up to LCFS region (r~76 – 74 mm). Observed suppression of the radial fluctuation induced flux

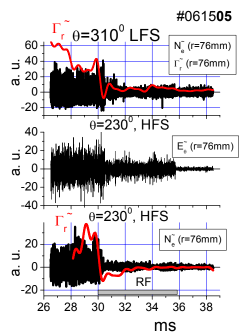

Fig. 2. The poloidal electric field $E_\theta^{\sim}$, density $N_e^{\sim}$ oscillations and the radial fluctuation induced flux $\Gamma_r^{\sim}(t)$ (red lines) near of the LCFS.

$\Gamma_r^{\sim}(t) = C_{n(\sim)E(\sim)}\, c\langle n^{(\sim)2}(t)\rangle^{1/2} \langle E_\theta^{(\sim)2}(t)\rangle^{1/2}/B_\varphi$, during LHH could be caused by damping of poloidal electric field $E_\theta^{\sim}$, and density $N_e^{\sim}$ oscillations as well as by the reduction of the correlation coefficients $C_{n(\sim)E(\sim)}$. Fig. 2 illustrates the time behaviour of these fluctuation parameters at plasma periphery for LCFS region ($r = 76mm$) at LFS ($\theta = 310^0$) and HFS ($\theta = 230^0$) (the quasistationary part of the signals are subtracted). Abrupt decrease on the radial density (see Fig. 3) and temperature profiles in the LCFS vicinity, together with that data rise measured by the laser Thomson scattering (TS) diagnostics and other diagnostics, shows that effective plasma LH heating and L – H transition results in decrease of the minor plasma radius and detaching of the plasma column from the limiter [4].

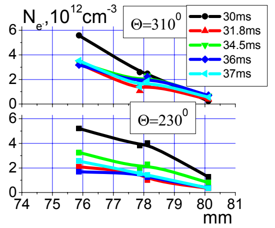

Fig. 3. The SOL plasma density profiles changes

The experimental data shows that the probe signals (see Fig. 2) have a burst structure indicating the registration by the Langmuir probes of turbulence waveforms with an density exceeding the density of the background plasma. According to model presented in [5] some filamentary plasma structure (filaments, blobs) with enhanced density and elongated shape along magnetic field lines are formed in vicinity of the LCFS. They are polarized and move to the chamber wall because of the $E_\theta \times B_\varphi$ radial drift. Time-correlated density and poloidal electrical field bursts could be interpreted as movement in radial direction of the filaments or blobs of intermittency transport. Because the bursts have varying amplitude and frequency of occurrence, a computer code for “Conditional Averaging” (CA) [6, 7] (as statistical method) was used to detect blobs propagating in the radial SOL direction as well as verify the correlation of different fluctuation events of the intermittency. The result of such CA treatment can be seen in Fig. 4. There are the denotation of the averaged bursts of the ion saturation current on the second pin ($I_s(2)$) and of difference in voltage (E_θ, V/cm) between two floating electrodes (denoted as (1) and (3) in Fig. 1) symmetrically shifted in the poloidal direction in respect to the electrode (denoted as (2)). The data obtained for two spatial points on the LFS (θ = 310^0) are shown in Fig. 4. Fig. 4a, 4b present the data for the radius r = 76mm and Fig. 4c, 4d for $r = 78mm$. The signal samples of 2 ms duration are analyzed with 1 MHz of digitization at two moments: before LH heating (L-mode, Fig. 4a and 4c) and

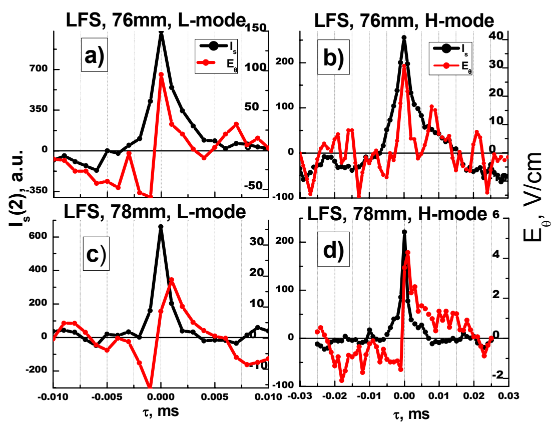

Fig.4 The conditional averaged ion saturation current ($I_s(2)$) and poloidal electric field E_θ.

on post-heating phase (H-mode, Fig. 4b and 4d). A threshold of 2.5σ (σ is RMS deviation) fluctuation level was chosen. All fluctuations with the relative amplitude above this level are detected as intermittent bursts. Positive and negative threshold levels were used. To be noted is that the negative I_s busts overdrawing the negative threshold level practically weren't observed. The temporal interval τ (x axis of the Fig. 4) is taken as averaged temporal intervals between of two neighboring bursts. It is centered at each burst maximum and then all detected bursts are averaged over the given time interval τ. The ion saturation current was used as the primary signal for CA. The other one (E_θ) was used as the secondary signal. CA was applied to signals measured in the radial range of 76 to 78mm. One can see from Fig 4, that positive bursts of the I_s or plasma density correlate with the positive fluctuations of the poloidal electric field. It corresponds to a radial drift towards to the wall. The averaged I_s positive signal is asymmetrical - there is an abrupt increase and a smooth decrease. An analogous form of the averaged peak was described in [6] and can be interpreted as the movement of plasma structures with a steep front followed by a long tail. The comparison of the data shows that average radial particle flux amplitude ($\Gamma_r \sim n\ E_\theta$) is decreased approximately one order of magnitude during L – H transition. It is visible that the frequency of bursts ($f = 1/\tau$) is decreased by about three times. The measurements on the HFS (θ=230^0) didn't show analogous formations. In that case there is not the well-defined burst of the CA E_θ, corresponding to the averaged intermittent burst of the I_s. So, the experiments show, that L – H transition initiated by effective LHH and accompanied by the radial fluctuation particle transport decrease results in drop of the intermittent "burst' transport on the LFS.

The spatial - temporal characteristics of the peripheral plasma fluctuations were investigated by Langmuir probe measurements using registration of signals from several spatial separated pins in vicinity of the LCFS. The distance between two floating electrodes in poloidal and radial directions was $\Delta r = 4.2mm$ [2]. Comparison of the corresponding pair of voltages from the floating electrodes allows to define the time lags (or phase velocity) of the signals in the poloidal and radial directions. The sample data for such treatment by mentioned above CA method are presented in Fig. 5. The data was obtained for the HFS ($\theta = 230^0$, $r = 78mm$) in the L-mode for pins arranged in the poloidal (f3 and f5) and radial (f1 and f3) directions. The figures permit to define the temporal lags $\Delta\tau$ and therefore the velocity $v = \Delta r/\Delta\tau$. According to the presented HFS data (Fig. 5a) the radial velocity of the extra burst of the floating potential ($\varphi_f - \overline{\varphi_f} > 2.5\sigma$) in the L-mode is found to be

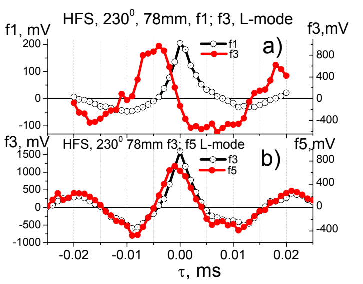

Fig. 5 CA data of the floating potential from electrode on the HFS in the L-mode for pins located in the poloidal (f3 and f5) and radial (f1 and f3) directions.

$v_r(r=78mm) \approx 0.8km/s$. The same data for $r=76mm$ leads to $v_r(r=76mm) \approx 1km/s$. After L-H transition the radial velocities are decreased about two times. The same dependences are observed for LFS. The poloidal velocity (to the ion diamagnetic drift direction), is accordingly Fig. 5b, $v_\theta(r=78mm) \approx 4km/s$. The observed time lags (≤ 1μs), unfortunately, are of the same order of magnitude than the time of digitization (1μs) of the analogue-to-digital converter. To increase of the accuracy of such measurements the new data acquisition system based on the 12th digit analogue-to-digital converter with 50MHz timing generator recently has been installed for probe signal registrations.

The first data with the new recorded system are presented in the Fig. 6, where the summery poloidal velocity $V_\theta = V_{\theta,\, phase} + V_{\theta,\, ExB}$ of the periphery plasma fluctuations (red line) are compared with $E_r x B_\varphi$ poloidal plasma drift velocity $V_{\theta,\, ExB}$ for a long-term period (from 18ms to 42ms) of the discharge. Here the poloidal velocity V_θ is obtained using time lags between signals of the floating electrodes (f3 and f5) calculated by cross-correlation method. Three prior conclusions could be done. (1) For both velocities there is change of the direction of the poloidal rotation from electron ($E_r<0$) to ion ($E_r>0$) diamagnetic drift direction at the early discharge phase. (2) During RF pulse (LHH) and post heating V_θ is decreased. It should be noted that the decrease of the poloidal velocity with L – H transition is in agreement with the results obtained early by treatment of data with 1μs digitization which are presented in [4]. (3) The poloidal velocities of peripheral plasma fluctuations V_θ and $V_{\theta,\, ExB}$ are very close at least from 27 up to 40ms, which point out at relatively small value of the $V_{\theta,\, phase}$. These data are under further treatment for more detailed analysis and must be used in future (together with other data) for conclusions about the nature of the peripheral turbulence and its parameters.

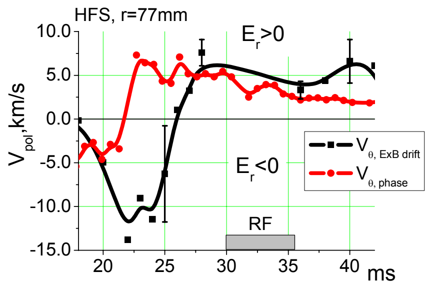

Fig.6 Comparison of the phase poloidal velocity of the periphery plasma fluctuations with $E_r x B_\varphi$ plasma drift poloidal velocity for long time period of the discharge.

This work was supported by RFBR 08-02-00610, 07-02-00895, 06-02-16785, INTAS Grant 05-8046, NSH-1550.2008.2 and "Rus. Science Support Foundation" grants.

References

1. S. I. Lashkul et al. Plasma Physics Reports, 2006, Vol. 32, No. 5, pp. 353–362.
2. S. V. Shatalin et al. Plasma Physics Reports, 2007, Vol. 33, No. 3, pp. 169–178.
3. S.I. Lashkul et al. 33rd EPS Conf. on Pl. Ph. Rome, 19 - 23 June 2006 Vol.**30I**, P-4.099
4. S.I. Lashkul et al. 34th EPS Conference on Plasma Phys. Warsaw, 2 - 6 July 2007, P-2.055
5. S.Krasheninnikov 2001 Phys. Lett. A **283** 368
6. Filippas A V et al 1995 Phys. Plasmas **2** 839
7. G S Kirnev, V P Budaev, S A Grashin et al Plasma Phys. Contr. Fusion 46 (2004) 621–637